



# Genomic Characterization and Copy Number Variation of *Bacillus anthracis* Plasmids pXO1 and pXO2 in a Historical Collection of 412 Strains

Angela Pena-Gonzalez,<sup>a</sup> Luis M. Rodriguez-R,<sup>d</sup> Chung K. Marston,<sup>b</sup> Jay E. Gee,<sup>b</sup> Christopher A. Gulvik,<sup>b</sup> Cari B. Kolton,<sup>b</sup> Elke Saile,<sup>b</sup> Michael Frace,<sup>c</sup> Alex R. Hoffmaster,<sup>b</sup> Konstantinos T. Konstantinidis<sup>a,d</sup>

<sup>a</sup>School of Biological Sciences, Georgia Institute of Technology, Atlanta, Georgia, USA

<sup>b</sup>Bacterial Special Pathogens Branch, Division of High-Consequence Pathogens and Pathology, National Center for Emerging and Zoonotic Infectious Diseases, Centers for Disease Control and Prevention, Atlanta, Georgia, USA

<sup>c</sup>Biotechnology Core Facility Branch, Division of Scientific Resources, National Center for Emerging and Zoonotic Infectious Diseases, Centers for Disease Control and Prevention, Atlanta, Georgia, USA

<sup>d</sup>School of Civil & Environmental Engineering, Georgia Institute of Technology, Atlanta, Georgia, USA

**ABSTRACT** *Bacillus anthracis* plasmids pXO1 and pXO2 carry the main virulence factors responsible for anthrax. However, the extent of copy number variation within the species and how the plasmids are related to pXO1/pXO2-like plasmids in other species of the *Bacillus cereus sensu lato* group remain unclear. To gain new insights into these issues, we sequenced 412 *B. anthracis* strains representing the total phylogenetic and ecological diversity of the species. Our results revealed that *B. anthracis* genomes carried, on average, 3.86 and 2.29 copies of pXO1 and pXO2, respectively, and also revealed a positive linear correlation between the copy numbers of pXO1 and pXO2. No correlation between the plasmid copy number and the phylogenetic relatedness of the strains was observed. However, genomes of strains isolated from animal tissues generally maintained a higher plasmid copy number than genomes of strains from environmental sources ( $P < 0.05$  [Welch two-sample *t* test]). Comparisons against *B. cereus* genomes carrying complete or partial pXO1-like and pXO2-like plasmids showed that the plasmid-based phylogeny recapitulated that of the main chromosome, indicating limited plasmid horizontal transfer between or within these species. Comparisons of gene content revealed a closed pXO1 and pXO2 pangenome; e.g., plasmids encode  $<8$  unique genes, on average, and a single large fragment deletion of pXO1 in one *B. anthracis* strain (2000031682) was detected. Collectively, our results provide a more complete view of the genomic diversity of *B. anthracis* plasmids, their copy number variation, and the virulence potential of other *Bacillus* species carrying pXO1/pXO2-like plasmids.

**IMPORTANCE** *Bacillus anthracis* microorganisms are of historical and epidemiological importance and are among the most homogenous bacterial groups known, even though the *B. anthracis* genome is rich in mobile elements. Mobile elements can trigger the diversification of lineages; therefore, characterizing the extent of genomic variation in a large collection of strains is critical for a complete understanding of the diversity and evolution of the species. Here, we sequenced a large collection of *B. anthracis* strains ( $>400$ ) that were recovered from human, animal, and environmental sources around the world. Our results confirmed the remarkable stability of gene content and synteny of the anthrax plasmids and revealed no signal of plasmid exchange between *B. anthracis* and pathogenic *B. cereus* isolates but rather predominantly vertical descent. These findings advance our understanding of the biology and pathogenomic evolution of *B. anthracis* and its plasmids.

Received 7 May 2018 Accepted 28 July 2018 Published 14 August 2018

**Citation** Pena-Gonzalez A, Rodriguez-R LM, Marston CK, Gee JE, Gulvik CA, Kolton CB, Saile E, Frace M, Hoffmaster AR, Konstantinidis KT. 2018. Genomic characterization and copy number variation of *Bacillus anthracis* plasmids pXO1 and pXO2 in a historical collection of 412 strains. *mSystems* 3:e00065-18. <https://doi.org/10.1128/mSystems.00065-18>.

**Editor** Rup Lal, University of Delhi

**Copyright** © 2018 Pena-Gonzalez et al. This is an open-access article distributed under the terms of the [Creative Commons Attribution 4.0 International license](https://creativecommons.org/licenses/by/4.0/).

Address correspondence to Alex R. Hoffmaster, amh9@cdc.gov, or Konstantinos T. Konstantinidis, kostas@ce.gatech.edu.

**KEYWORDS** *Bacillus anthracis*, anthrax-like *B. cereus*, pXO1, pXO2, pathogenomics, phylogenomics

*Bacillus anthracis*, the etiological agent of anthrax, is a Gram-positive endospore-forming bacterium belonging to the *Bacillus cereus sensu lato* group (1, 2). Dormant spores represent the infecting form of the bacterium and can remain viable in soils for decades (3–6). *B. anthracis* has two circular, extrachromosomal DNA plasmids, pXO1 and pXO2, which carry the major virulence factors required for pathogenesis (6, 7). pXO1 carries the genes that encode the following anthrax toxin proteins: protective antigen (PA), lethal factor (LF), and edema factor (EF). These proteins act in binary combinations to produce the two anthrax toxins edema toxin (PA and EF) and lethal toxin (PA and LF) (6–9). Plasmid pXO2 harbors the genes that encode the *cap* operon responsible for the production of a polyglutamate capsule, which allows the pathogen to evade the host immune response by protecting itself from phagocytosis (6–9).

Given the severity of the disease and the fact that this microorganism can be used as a biological weapon, it is important to characterize the diversity of the two virulence plasmids in a large collection of strains. Currently, plasmid detection is mainly accomplished by amplification of specific markers through PCR (7, 10). Although this approach is relatively rapid, it can miss plasmids that have diverged in sequence and cannot reveal the full gene content of plasmids. In addition, the plasmid copy number and the extent of copy number variation among members of *B. anthracis* are still unclear. For example, by using quantitative PCR (qPCR), Coker et al. reported ratios of up to 40.5 copies of plasmid pXO1 and 5.4 copies of plasmid pXO2 per genome (8), while Pilo et al. reported 10.89 as the average number of copies for pXO1 and 1.59 for pXO2 (11). Using digital PCR (dPCR) in analyses of three isolates, Straub et al. reported that there are likely 3 to 4 copies of pXO1 per cell and 1 to 2 copies of pXO2 (12). Sequence-based projects have also revealed that there are likely 2 to 3 copies of pXO1 per chromosome copy (13). An important limitation in those previous estimates was that they were performed with a relatively small number of isolates, which can bias the characterization of the population copy number variation. In addition, previous studies have suggested that the virulence levels of *B. anthracis* strains carrying both plasmids can differ depending on the copy number of the plasmids (8). These results underscore the necessity to accurately quantify plasmid copy variation in a large collection of diverse *B. anthracis* isolates and evaluate whether plasmid copy number is a phylogenetically conserved trait. High-throughput, sequence-based methods not only can detect and quantify plasmid copy number but also can elucidate gene content and sequence diversity, which ultimately will allow better understanding of the pathogenomic evolution within the group and with other close relatives. Several studies have already characterized the phylogenetic relationships and population structure of hundreds of *B. anthracis* isolates in France, the Netherlands, and the United States using high-resolution, sequence-based methods such as those analyzing single nucleotide polymorphisms (SNPs) (1–3). The major results from these studies have shown that *B. anthracis* isolates are highly clonal with remarkably stable genomes and low intraspecies diversity and can be placed into 1 of 12 conserved lineages defined by canonical SNPs (CanSNPs). However, no studies to date have focused on characterizing plasmid diversity and copy number variation in large *B. anthracis* data sets.

Further, the *B. anthracis* genome, despite its observed stability, is rich in mobile elements (transposases, resolvases, and integrases), which could be an important factor in plasmid gene content diversification and horizontal transfer (14). Whether or not the pXO1 and pXO2 plasmids are mobile and can be transferred between *B. anthracis* genomes as well as to and from other members of the *Bacillus cereus sensu lato* group remains speculative, but that issue might be directly related to the virulence of the genomes and the evolutionary history of the plasmids. Gene transfer and deletion are also important for classification since these species are typically classified based on their plasmid and virulent factor content (as opposed to phylogeny) in this group.

Finally, the phylogenetic relationships within the *Bacillus cereus sensu lato* group are still problematic. *B. anthracis* belongs to the *B. cereus sensu lato* group, which also includes two other main species: *B. cereus sensu stricto* and *B. thuringiensis* (15, 16). These species were initially recognized and established because they exhibited the following distinct phenotypic traits: *B. anthracis* was identified as the causative agent of anthrax (15); *B. thuringiensis* was recognized as an entomopathogenic bacterium characterized by the production of parasporal crystal proteins (Cry and Cyt), which have been widely used as a natural pesticide (16); and finally, *B. cereus sensu stricto*, initially recognized as a common soil-dwelling microorganism, colonizes the gut of invertebrates as a symbiotic microorganism and is also an opportunistic human pathogen (17, 18). DNA hybridization techniques, 16S rRNA-based typing, and multilocus sequence typing (MLST) schemes have progressively revealed limited genomic dissimilarities existing among these species, demonstrating that they are more closely related than had initially been considered (19). This, and the fact that the main phenotypic traits for classification are carried in plasmids, has led to discussion on whether or not the members of the *B. cereus sensu lato* group should be considered a single species with characterized ecotypes and pathotypes (16, 19).

Therefore, full-genome analysis of newly sequenced *B. anthracis* strains and representative strains in the *B. cereus sensu lato* group is critical to further elucidate the true phylogenetic relationships within the group. In addition, *B. cereus* strains encoding genetic determinants that confer pathogenic capabilities similar to those of *B. anthracis* have been described previously (20–24). Marston et al. (20) and Hoffmaster et al. (21) reported the isolation of *B. cereus* strains producing anthrax-like diseases in humans with clinical presentations of pneumonia and cutaneous lesions in North America, respectively. More recently, Antonation et al. reported the collection of four atypical *B. cereus* isolates (designated *B. cereus* bv. *anthracis*) from dead mammals (chimpanzees, gorillas, elephants, and goats) in west and central Africa (23). These isolates harbored virulence plasmids similar to those of the *B. anthracis* Ames strain. We have also recently described the genome of *B. cereus* strain LA2007, a human-pathogenic isolate carrying a pXO1-like plasmid that showed 99.70% average nucleotide identity (ANI) to *B. anthracis* Ames pXO1 (25). Interestingly, the pXO1-like plasmids of the pathogenic *B. cereus* strains reported to date are similar but not identical to those found in *B. anthracis*. Therefore, determining the genetic backbone and phylogenetic diversity of the pXO1/pXO2-like plasmids is critical, not only to develop more accurate detection tools, but also to understand the pathogenomic evolution of virulence determinants within the *B. cereus sensu lato* group.

In this study, we used next-generation sequencing data to detect, quantify, and characterize the full genomic content of *B. anthracis* plasmids pXO1 and pXO2 in a collection of 412 newly sequenced strains that represent the global diversity of the species recovered to date. We also compared the phylogenetic diversity of *B. anthracis* representatives with that of a set of 106 available/reference *B. cereus sensu lato* strains that included nonpathogenic strains as well as pathogenic strains carrying pXO1-like plasmids.

## RESULTS

**Estimated plasmid copy number and covariance.** In this study, a total of 412 *B. anthracis* strains were newly sequenced. The results of the whole-genome comparison of these genomes will be reported elsewhere; here, we focused our analyses on the plasmid sequences. The libraries had an average sequencing depth of 135.4 $\times$ , with a median value of 128.3 $\times$  and a minimum value of 9.8 $\times$ . To estimate pXO1 and pXO2 copy numbers, we calculated the ratio of plasmid sequence depth (using *B. anthracis* Ames ancestor plasmid sequences as references to recruit reads) to the average sequencing depth for the chromosome. We identified a total of 58 and 42 strains that completely lacked pXO1 and pXO2, respectively, or that had too few reads (i.e., <2 $\times$  sequencing depth after subsampling; see Materials and Methods for details) mapping on the plasmid (i.e., 42 and 62 strains for pXO1 and pXO2, respectively) and that were

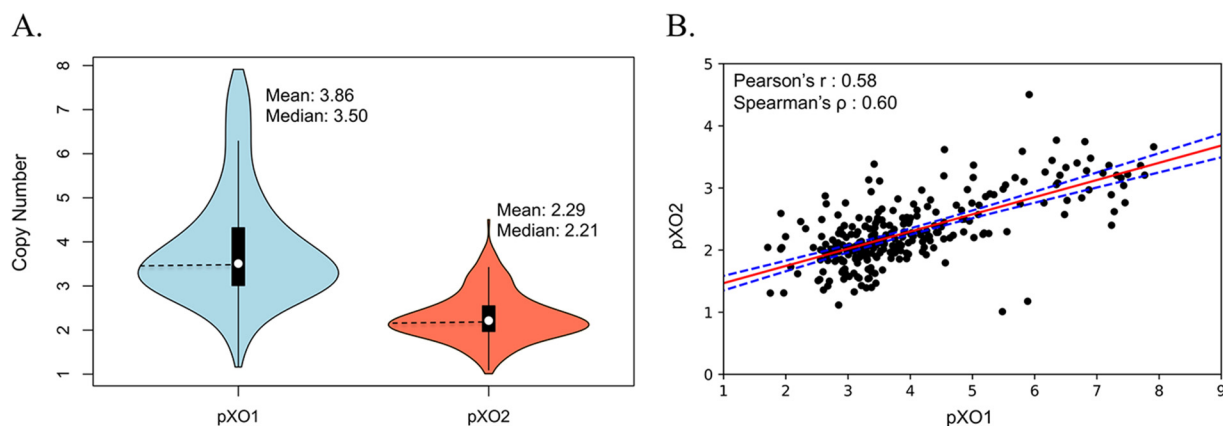


**FIG 1** Copy number estimation for *Bacillus anthracis* plasmids pXO1 and pXO2. (A) Plasmid copy number distribution calculated for strains carrying one or both plasmids. *B. anthracis* cells maintain an estimated average of 3.86 copies of plasmid pXO1 and 2.29 copies of plasmid pXO2, indicating a general pattern where the copy number of pXO1 is nearly twice (1.68 $\times$ ) that of pXO2. (B) Correlation analysis of pXO1 and pXO2 estimated copy numbers showed a high degree of linear positive correlation (Pearson's  $r = 0.68$ , Spearman's  $\rho = 0.62$ ). The red line indicates the estimated linear regression model, and the dashed blue lines depict the upper and lower confidence intervals at 95%.

therefore not included in the estimations. By calculating the ratio of plasmid sequencing depth to chromosome sequencing depth, we estimated that *B. anthracis* cells maintain on average 3.86 copies of plasmid pXO1 (standard deviation [Stdev] = 1.27) and 2.29 copies of pXO2 (Stdev = 0.54), indicating a general pattern in which there are almost twice (1.68 times) as many copies of pXO1 relative to pXO2 (Fig. 1A). In addition, we observed a large variation in copy number where some strains carried up to 7.8 copies of pXO1, contrasting with pXO2, where the maximum number of copies was 4.5 and was generally less variable. We also observed a considerable degree of positive linear correlation between the copy numbers of pXO1 and of pXO2 (Pearson's  $r = 0.68$ , Spearman's  $\rho = 0.62$ ) (Fig. 1B).

**Plasmid copy number variation and genomic relatedness.** Next, we evaluated whether plasmid copy number in *B. anthracis* is a phylogenetically conserved trait. To test this hypothesis, we calculated the Blomberg's  $K$  statistics (26), which relate the amount of phylogenetic signal present in comparison to the expected amount under conditions of Brownian motion of character evolution as calculated using a dendrogram derived from an ANI distance tree (Fig. 2). We observed no correlation between the plasmid copy number and genome average nucleotide identity (ANI) distances among strains (Blomberg's  $K = 0.013$  for pXO1 and  $K = 0.014$  for pXO2; Fig. 2), indicating that plasmid copy number is not phylogenetically conserved. Thus, closely related strains do not necessarily carry similar plasmid copy numbers.

**Plasmid copy number and source of isolation.** To evaluate any correlation existing between the estimated plasmid copy number and the source of the strains, a comparative analysis was performed on 127 strains for which biological source information was available. The biological source was defined as human, animal, or environmental based on the sample from which each strain was isolated. Isolates included in the environmental group were obtained from different nonclinical-, non-animal-associated sources, including but not restricted to soil. Several of the environmental isolates were also recovered from swabs that had been applied to surfaces within mills, warehouses, or other facilities that processed animal products (e.g., yarn, hair, bone, bone meal, etc.) (see Biosample accession number in Table S1 in the supplemental material). Results showed that *B. anthracis* isolated from human and animal sources generally maintained a higher plasmid copy number than strains isolated from environmental sources ( $P = 9.7e-5$  for pXO1 and  $P = 0.05$  for pXO2 [Welch two-sample  $t$  test]) (see Fig. S2 in the supplemental material). To exclude the possibility that this observation was the result of DNA extraction method, given that two protocols were implemented (Qiagen and Promega; see Materials and Methods for further details), we

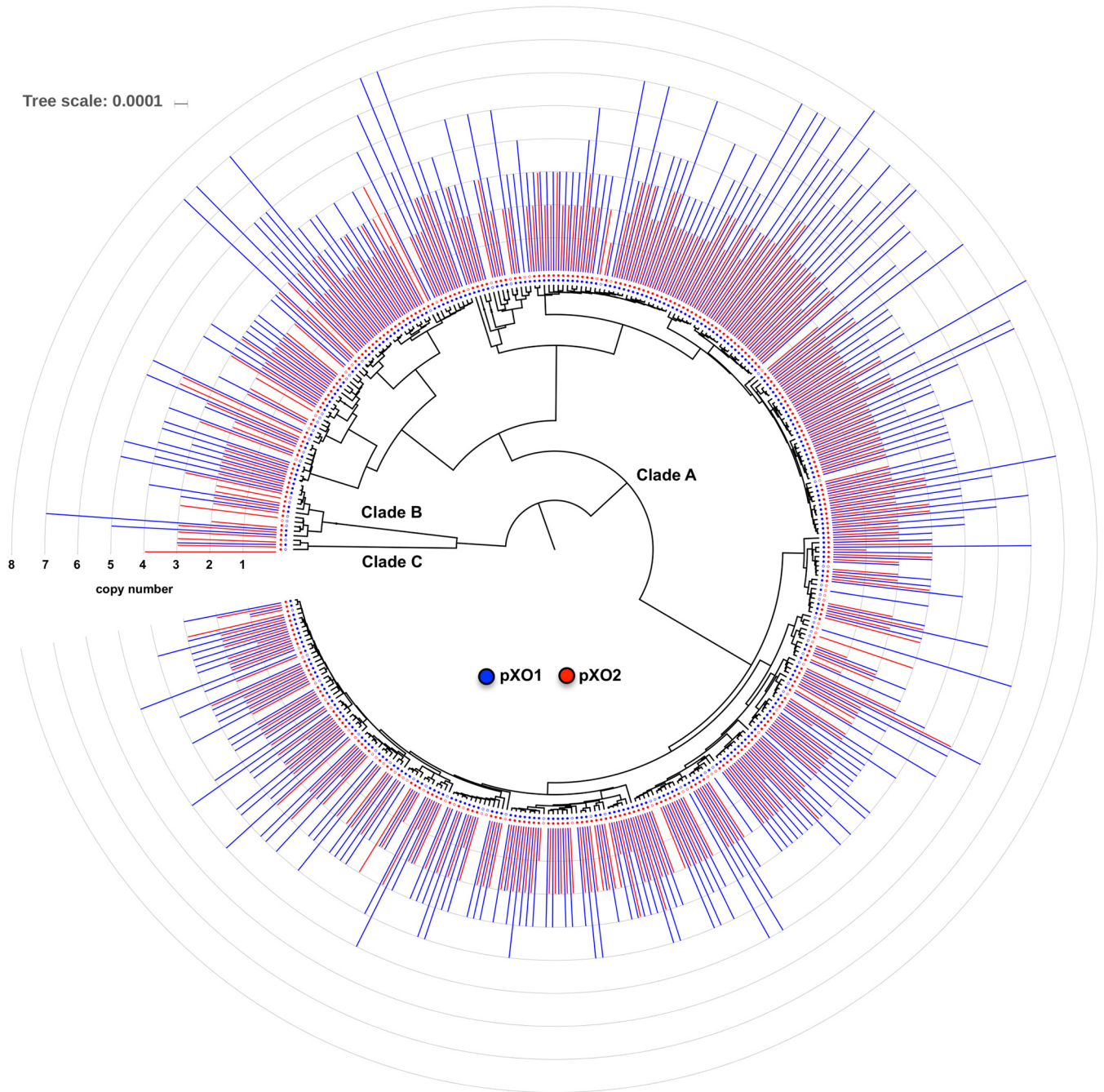


**FIG 2** Lack of phylogenetic conservatism of *Bacillus anthracis* plasmid copy number. A dendrogram was constructed based on the average nucleotide identity (ANI) distances calculated for 412 *B. anthracis* strains. Presence or absence of pXO1 (inner circle in blue) and pXO2 (inner circle in red) and estimated plasmid copy number data (bar plots) are shown. Strains with high and low plasmid copy numbers were found to be dispersed across the three main clades, i.e., clade A ( $n = 397$ ), clade B ( $n = 12$ ), and clade C ( $n = 3$ ), and no apparent clusters were evident. The tree scale corresponds to 1 – ANI distance.

performed a two-sample  $t$  test analysis comparing plasmid copy numbers between the two extraction methods. The results revealed no significant difference ( $P = 0.11$  for pXO1 and  $P = 0.81$  for pXO2). In addition, we performed an analysis of variance (ANOVA) to determine the influence of DNA extraction method and biological source (two independent variables) in explaining the values of plasmid copy number (the continuous dependent variable). The results showed that the variation explained by the biological source was significant ( $F = 6.23$ ,  $P = 0.01$ ) whereas the variation explained by the extraction method was not ( $F = 0.072$ ,  $P = 0.7$ ).

**Plasmid-based versus chromosome-based phylogenetic relationships.** To determine whether plasmid-based ANI clustering resembled that shown by the chromosome, we analyzed strains for which plasmid pXO1 and/or pXO2 were detected, in addition to incorporating 36 *B. anthracis* reference strains that were sequenced previously (see Table S2 and Table S3). Initial characterization of genomic relatedness based on the ANI distance values determined for the chromosome showed that the strains in the total set were grouped in three main clades: clade A (397 strains), clade B (12 strains), and clade C (3 strains), with clade A containing the majority of strains, similarly to what has been previously described with other typing methods such as multilocus variable-number tandem-repeat analysis (MLVA) (Fig. 2). When we compared the clustering profiles of both plasmids versus that of the chromosome, we observed a high level of topological correlation. To quantify the strength of the correlation we used two metrics: (i) the cophenetic distance, defined as the intergroup distance at which two observations are first combined into a single cluster, and (ii) the Baker's  $\Omega$  index, defined as the rank correlation between the stages at which the pairs of observations combine in each one of the two dendrograms being compared. For pXO1, the calculated cophenetic correlation was 0.70, and the Baker's  $\Omega$  index correlation was 0.62. For pXO2, the calculated cophenetic correlation was 0.89, and the Baker's  $\Omega$  correlation was 0.93, indicating that, in general, the pXO1 and pXO2 phylogenies recapitulate that of the chromosome.

**Gene content variation of pXO1 and pXO2.** To avoid limitations of the assembly process, such as gaps or truncated genes and misassemblies, we assessed gene content variations of the plasmids by recruiting high-quality (trimmed) Illumina reads against the predicted genes on the plasmid and determining gene presence/absence by the number of reads recruited (or not) on the gene. In general, genomes containing one or both plasmids showed highly conserved gene content (Fig. 3A and B). The calculated pXO1 pangenome was composed of 197 orthologous genes; 179 (91%) of them were present in all strains (strict core), and 195 (99%) were present in at least 95% of all the strains (relaxed core). Only two genes were found to be variable in pXO1. These genes were annotated (using the nonredundant UniProtKB/SwissProt databases) as a transposase for insertion sequence (IS) element IS231E (reported previously in *Bacillus thuringiensis* serovar finitimus) and G-protein-coupled receptor 98. In pXO2, 108 genes composed the pangenome; 96 genes were part of the strict core (89%), while 102 genes were part of the relaxed core. Only six genes composed the variable genome. Three of the six variable genes were annotated as encoding uncharacterized/hypothetical pXO2 proteins, two genes were annotated as encoding putative pXO2 *trans*-acting regulators, and one gene had partial homology (query coverage = 35%, identity = 45%) to the gene encoding subunit *ssr1* of the chromatin structure remodeling complex (RSC). All variable genes had hypothetical or poorly characterized functions or were mobile elements (e.g., transposases). Although the plasmid gene content diversity generally observed between any two genomes analyzed was not large, we identified a large fragment deletion in the pXO1 plasmid of one strain, i.e., strain 2000031682 (Fig. 3C). The deleted fragment was about ~46.3 kbp in length and contained 39 genes in total, including the following genes encoding the main virulence factors responsible for anthrax toxin: *cya*, *pagA*, *lef*, and the *atxA* transcriptional activator gene. We also identified a number of genes encoding integrases, resolvases, and transposases in and around the deleted fragment (Fig. 3D). Resequencing and reassembling of the strain confirmed the large gene deletion. In addition, we identified orthologous genes present in both plasmids that showed sequencing depth levels greater than those seen with the majority of plasmid genes. These genes were most likely multicopy genes. In pXO1, we identified three multicopy genes that were observed to have two copies, on average, consistently across the complete set of strains. In pXO2, we identified three genes with a consistent multicopy pattern in most of the strains characterized in this analysis. In both plasmids, these genes corresponded to transposases for insertion sequence elements (IS231F, IS231C, IS231B, IS231E, IS231A, and IS1151).

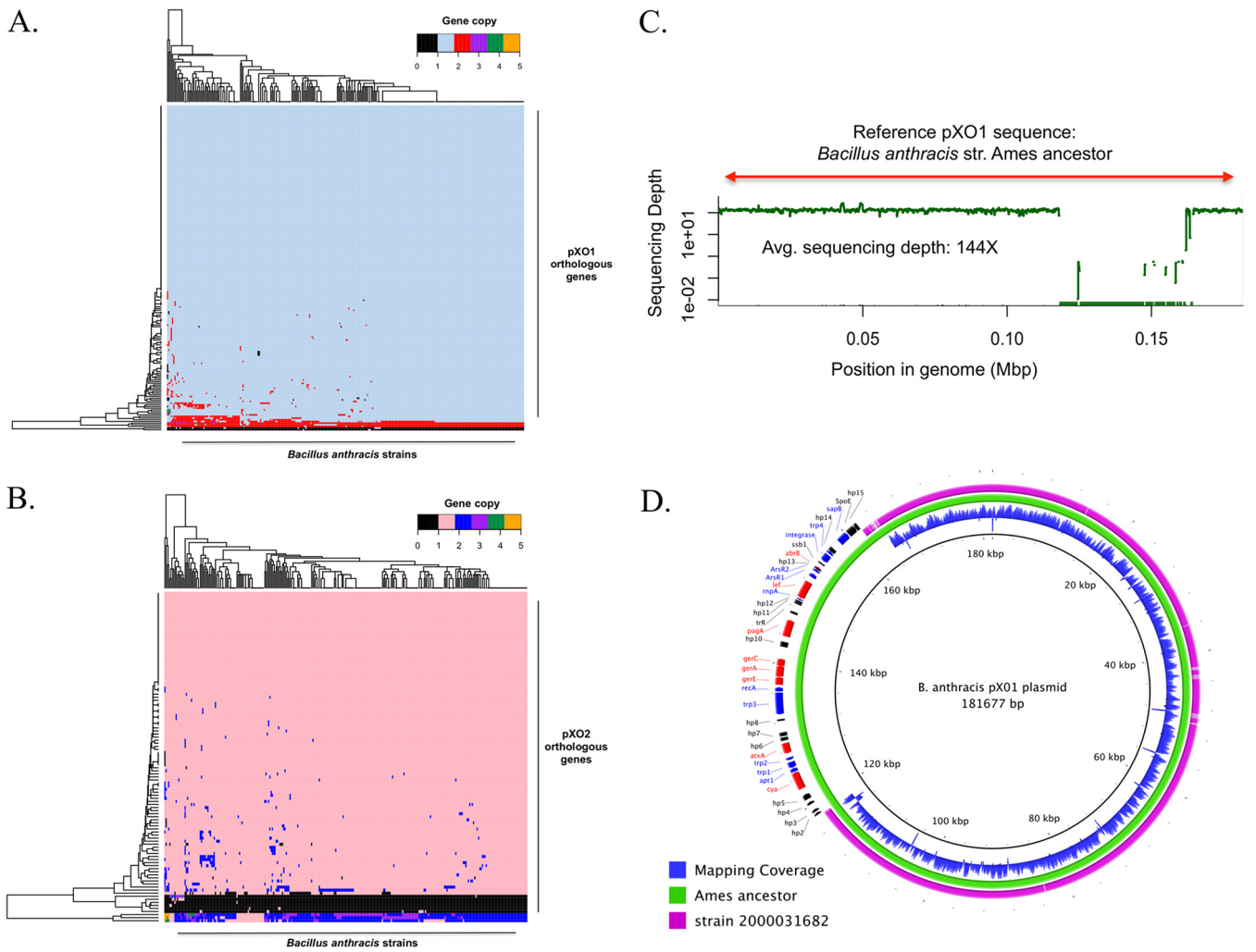


**FIG 3** Gene content variation of pXO1 and pXO2. (A) Hierarchical clustering of *B. anthracis* strains containing plasmid pXO1 (columns) based on the estimated sequencing depth for each representative orthologous gene (rows) normalized by the median sequencing depth for each genomic library (columns). (B) Data were determined as described for panel A but for plasmid pXO2. (C) Read recruitment plot showing the absence of read coverage in a region of ~46.3 kbp, while the calculated average sequencing depth of the covered region was 144 $\times$ . (D) Circular plot comparing pXO1 in *B. anthracis* strain Ames ancestor (in green) and in strain 2000031682 (in purple). Mapping coverage from sequencing reads of strain 2000031682 along the plasmid is shown in blue (innermost circle). The deleted fragment is shown along with the functional annotation of the genes identified in the region. Red arrows denote the position and strand of anthrax virulence determinant genes identified in the missing region, blue arrows identify mobile elements, and black arrows denote genes encoding hypothetical proteins.

**Comparison to pXO1/pXO2-like plasmids of other members of the *B. cereus sensu lato* group.** To increase understanding of the evolutionary relationships of *B. anthracis* plasmids with those of other (non-*B. anthracis*) members of the *B. cereus sensu lato* group, we performed an ANI-based clustering analysis of selected strains from our data set together with available reference *B. cereus sensu lato* strains. The final set included 94 *B. cereus* strains, 11 representative *B. anthracis* strains identified from our data set (medoids; see Materials and Methods), 11 *B. thuringiensis* strains, and 1 *B. mycooides* strain (see Table S2). Results showed that strains clustered in 3 main groups: clade I, clade II, and clade III (Fig. 4A). Representative strains from *B. anthracis* were grouped in clade I, the same group containing several *B. cereus* isolates of clinical origin. The majority of *B. thuringiensis* strains (7 of 11) were grouped in cluster III, although four of them were assigned to clade I. These relationships were consistent with previous phylogenetic characterizations based on MLST schemes or chromosomal core proteins, which have shown that *B. cereus*, *B. mycooides*, and *B. thuringiensis* are not confined within discrete clades and are, therefore, not monophyletic species (7–29).

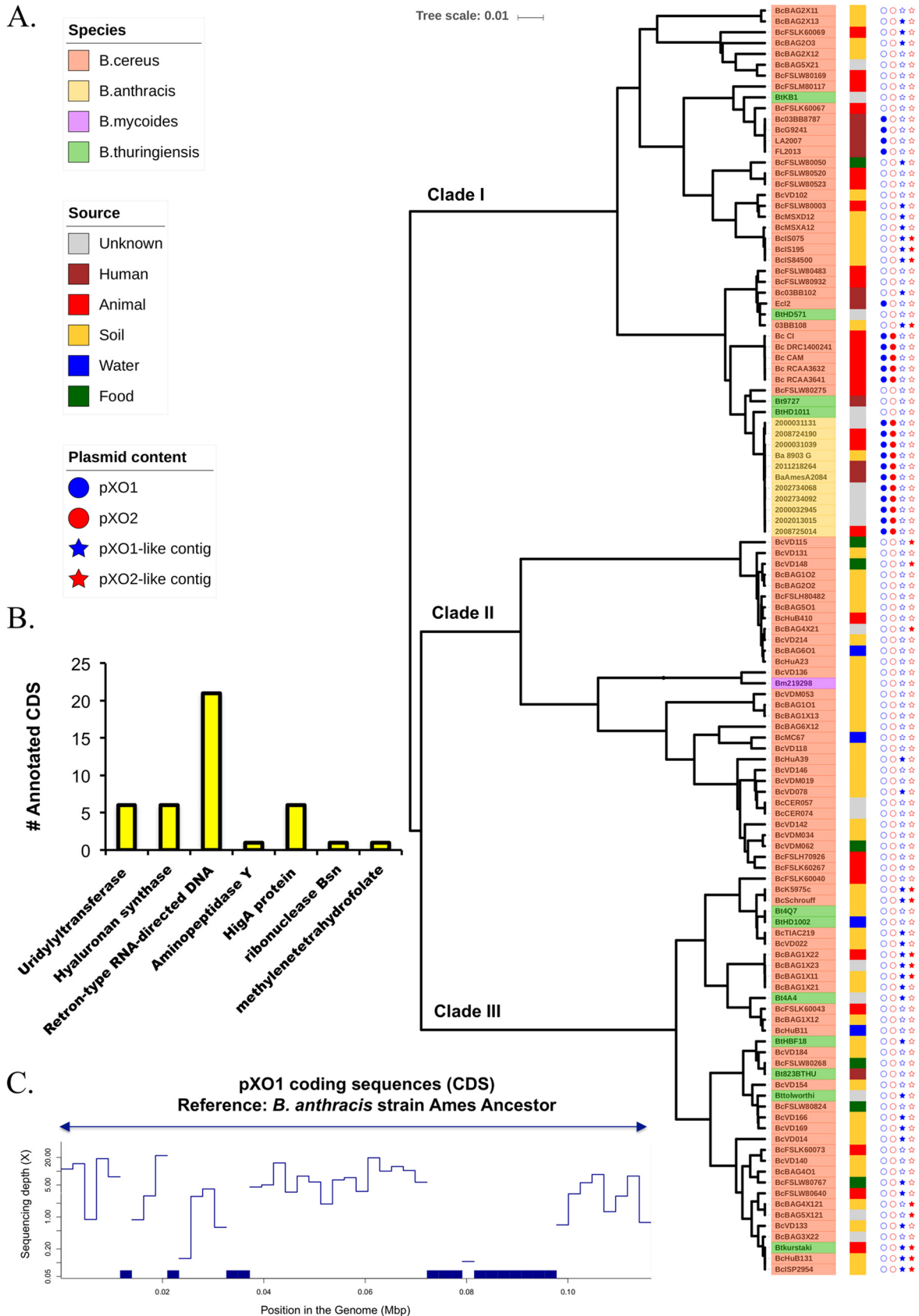


**FIG 4** Genomic characterization of *Bacillus cereus sensu lato* group. (A) Clustering of species within the *Bacillus cereus sensu lato* group based on ANI distances. *B. anthracis* members are colored in yellow; *B. cereus sensu stricto* strains are colored in pink; *B. thuringiensis* (Continued on next page)



We then attempted to identify non-*B. anthracis* genomes that carried a complete or partial genomic backbone with pXO1 and/or pXO2. To achieve this goal, since our genome sequences were incomplete (draft), we followed two approaches. First, we identified large ( $\geq 500$ -bp) contigs with  $\geq 80\%$  identity and  $\geq 80\%$  sequence coverage with respect to reference pXO1 and pXO2 plasmids from the *B. anthracis* Ames ancestor (we called these contigs “pXO1/2-like contigs”); second, we generated read recruitment plots to visualize and quantify the sequencing depth coverage provided by reads of the genomic library of the corresponding strain along with the reference plasmid sequence (see Materials and Methods). We identified 33 genomes containing pXO1-like contigs, 12 of which were assignable to clade I, 2 to clade II, and 20 to clade III. We also identified 17 strains containing pXO2-like contigs; 4 were assignable to clade I, 3 to clade II, and 10 to clade III (see, e.g., Fig. 4A). Functional characterization of the genes predicted in pXO1-like contigs (365 in total) showed that the majority of those genes corresponded to hypothetical proteins (97%) and that only 42 (3%) could be functionally annotated. Among these, five genes encoded hyaluronan synthase (Fig. 4B). In addition, we screened our *B. cereus sensu lato* data set for the *hasABC* operon and found that, among 116 genomes, only 11 strains harbored the functional gene set. These 11 genomes corresponded to pathogenic *B. cereus* strains (03BB87, 03BB102, CAM, CI, RCA-A-364-1, RCA-A-363-2, DRC14-0024-1, FL2013, LA2007, G9241, and Elc2). In all cases, the genes were colocated, and the *hasA* gene for strain Elc2 was the most divergent one (see Fig. S6). However, no anthrax toxin genes were identified among these sequences.

We also included in this analysis 11 previously characterized pathogenic *B. cereus* genomes carrying complete pXO1 and/or pXO2 plasmids. In particular, five *B. cereus* bv. *anthracis* strains (RCA\_A\_364-1, RCA\_A\_363-2, DRC\_14-0024-1, CAM, and CI) were isolated from dead mammals (chimpanzees, gorillas, elephants, and goats) with an illness consistent with anthrax in west and central Africa (23), and six pathogenic *B. cereus* strains (G9241, BcFL2013, LA2007, 03BB87, 03BB102, and Elc2) were isolated from human cases of pneumonia or cutaneous lesions. These strains were compared to 11 representative *B. anthracis* genomes (from our data set) and to an additional *B. cereus* strain (03BB108, isolated from dust at a worksite where a Texas welder contracted fatal pneumonia in 2003) that carried partial homology to the backbone of pXO1. Clustering analysis based on ANI dissimilarity revealed four groups (Fig. S3A). The first group was highly clonal and was composed of *B. anthracis* strains with an average intragroup ANI distance of 0.04 (i.e., 99.96% identity). The second group contained *B. cereus* bv. *anthracis* isolates which were also highly similar, with an average ANI distance of 0.03. The third group, labeled *B. cereus* group I, was composed of three *B. cereus* isolates (03BB108, 03BB102, and Elc2) that had among them an average ANI distance of 1.01. Finally, the fourth group, labeled *B. cereus* group II, was composed of four human-pathogenic *B. cereus* strains (LA2007, BcFL2013, G9241, and 03BB87) and showed an average of a 0.01 intragroup ANI distance, representing the smallest observed intragroup diversity value. *B. cereus* group II was the most divergent from all other groups, with an average intergroup ANI distance of 5.27 (Fig. S3B).

Plasmid detection and quantification based on read coverage confirmed that all *B. cereus* bv. *anthracis* strains carried complete pXO1-like and pXO2-like plasmids, while strains BcFL2013, G9241, 03BB87, LA2007, and Elc2 harbored a complete pXO1-like plasmid but not a pXO2-like plasmid (Fig. S3C). 03BB102, which was isolated from a patient with a fatal case of pneumonia in Texas, differed from the other strains in that it did not harbor a full-length pXO1-like or pXO2-like plasmid, although partial se-

#### FIG 4 Legend (Continued)

members are colored in green; and *B. mycooides* is colored in purple. The right colored strip indicates the source of isolation. Filled or empty circles indicate the presence (filled) or absence (empty) of pXO1 (in blue) and pXO2 (in red). Filled stars denote the strains for which pXO1-like (blue) or pXO2-like (red) contigs were identified. (B) The number of functionally annotated coding sequences (excluding hypothetical sequences) predicted in pXO1-like contigs (42 in total, 3% of the total number). (C) Example of *B. cereus* strain VD014 showing partial pXO1-like backbone homologous to pXO1 from *B. anthracis* Ames ancestor.

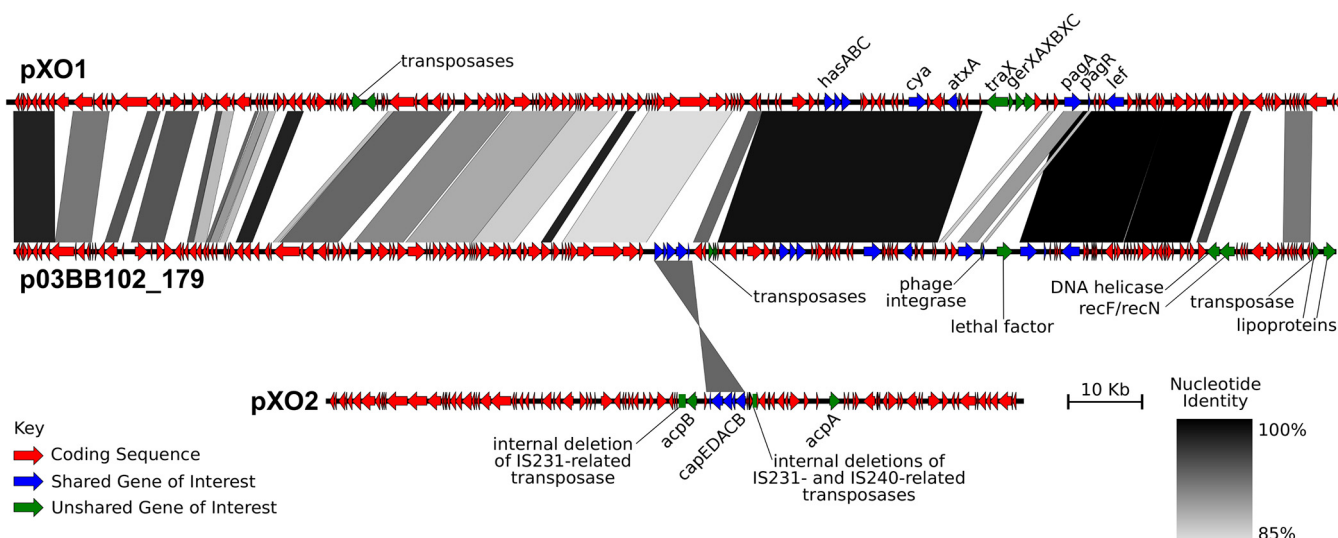


**FIG 5** Gene content comparison between *B. anthracis* pXO1/pXO2 and *B. cereus* strain 03BB102 plasmids. The connecting lines show the presence and location of shared genes, while the gray scale represents the level of nucleotide identity. p03BB102 carries a *cap* locus (~5.1 kbp) that shows 93% nucleotide identity to the *cap* locus in reference plasmid pXO2 (*B. anthracis* “Ames ancestor”; GenBank accession number [AE017335](#)) and is flanked by IS elements. A duplicate homolog of *pagA* and *pagR* genes is also present in p03BB102, with one homolog showing 99% identity to its pXO1 *B. anthracis* homolog (*B. anthracis* “Ames ancestor” GenBank accession number [AE017336](#)) for both genes, while the second shows 92% and 94% identity, respectively.

quence homology to the pathogenicity island was detected (51.72% of the total genes of the island were present) (22). Sequence-based analysis revealed that 03BB102 harbors the typical anthrax virulence genes but lacks about half of the canonical pXO1 gene content (Fig. S3C). Further gene-based characterization showed that this plasmid (p03BB102) carried a complete, 5.1-kbp pXO2 *cap* locus with 93% nucleotide identity to the Ames strain *cap* locus (GenBank accession number [AE017335](#)) and was flanked by 5 IS elements. In addition, duplicate homologs of protective antigen genes (*pagA* and *pagR*) were identified; one homolog showed ~99% nucleotide identity to its ortholog in pXO1 of the Ames ancestor strain, while the second showed 92% and 94% (respectively), indicating that these homologs have already begun to diverge (Fig. 5). Although pXO1/pXO2-like plasmids seem to be remarkably conserved in terms of gene content and synteny, strain 03BB102 is an exception to this rule, which suggests that the level of plasmid diversity in nature may be higher than previously thought.

We also calculated plasmid copy numbers in the set of *B. cereus* strains carrying *B. anthracis*-like plasmids (Table S1). The estimated average pXO1 copy number in *B. cereus* bv. *anthracis* strains was 1.8, while that for the set of human-pathogenic *B. cereus* strains was 2.32, which was similar to the estimated average for *B. anthracis* (3.86). For pXO2, the estimated average copy number in *B. cereus* bv. *anthracis* was 2.12, which is similar to the estimated copy number in *B. anthracis* (2.29).

**Assessing origins and vertical versus horizontal transmission of plasmids.** To determine if the pXO1/pXO2-like plasmids have been transferred between members of *B. cereus* and *B. anthracis*, we contrasted the phylogenetic relationships among the genomes on the basis of comparisons of the chromosomal genes to those of the plasmids. Phylogenetic reconstruction based on plasmid core orthologous genes of the strains harboring a complete pXO1 plasmid (139 genes) and/or pXO2 plasmid (88 genes) showed a topology similar to that observed with whole-genome ANI distance evaluations based on tanglegram analysis (Fig. 6), indicating limited lateral mobilization of the plasmids between the strains (Fig. S4). For pXO1, *B. cereus* bv. *anthracis* strains were closer to those in the *B. anthracis* group than they were to the set of human-pathogenic *B. cereus* group II strains, and Elc2 was the most divergent strain. For pXO2, three main clades were observed: (i) one containing all *B. anthracis* strains, (ii) another containing strain *B. cereus* CI, and (iii) a final clade containing the remaining *B. cereus* bv. *anthracis* strains (RCA\_A\_364-1, RCA\_A\_363-2, DRC\_14-0024-1, and CAM) (Fig. S4D).

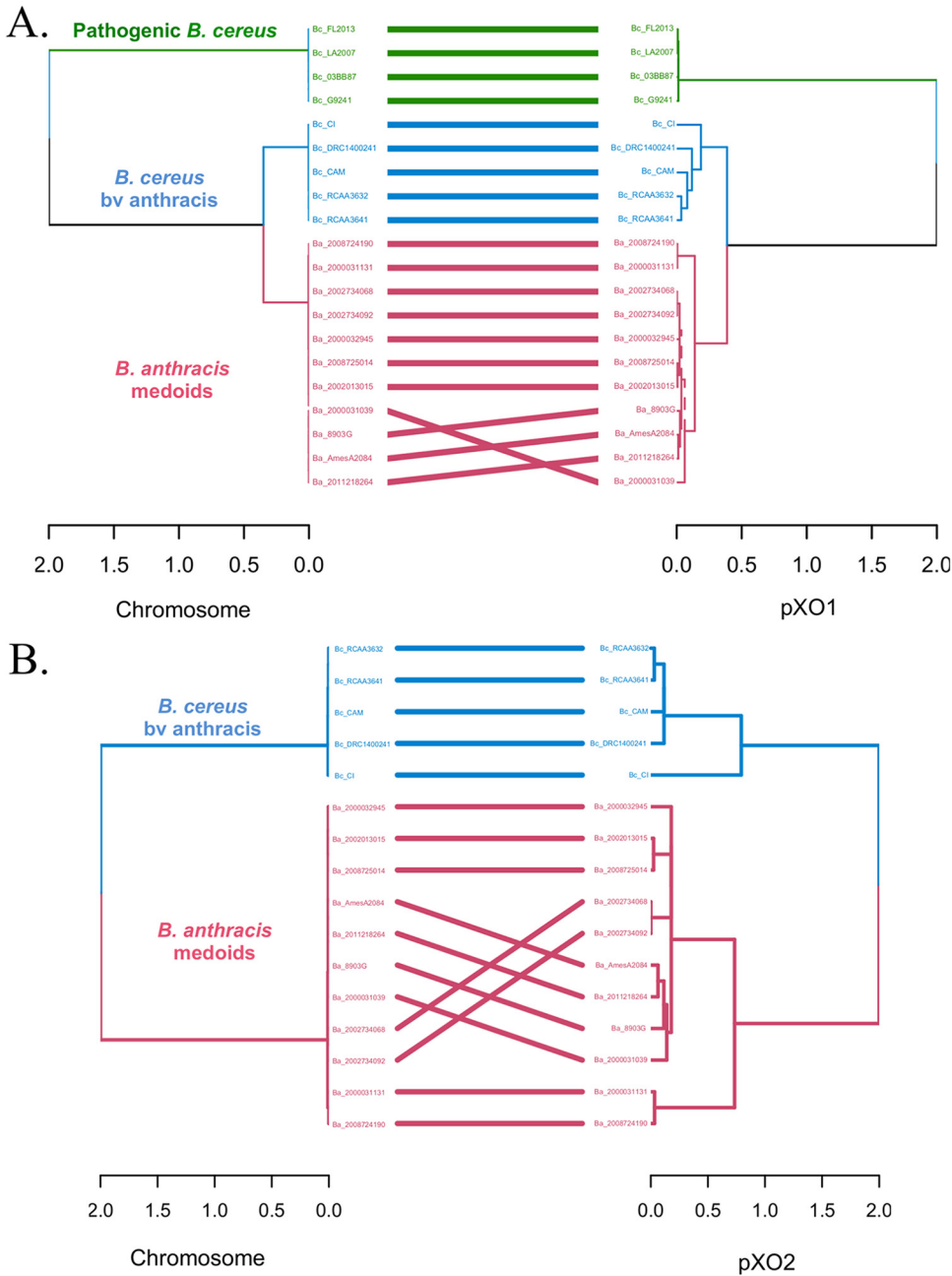


**FIG 6** Assessment of plasmid lateral transfer between representative *B. anthracis* and pathogenic *B. cereus* strains carrying complete pXO1/pXO2-like plasmids. (A and B) Comparison of phylogenetic relationships based on the core genome for the chromosome and pXO1 (A) and for the chromosome and pXO2 (B) in strains carrying one or both plasmids. Phylogenetic reconstructions shown in panel A were based on the alignment of 210,123 variable positions found in the concatenated alignment of 4,233 core orthologous genes for the chromosome and 458 variable positions identified in the concatenated alignment of 149 pXO1 core orthologous genes. Phylogenetic relationships in panel B were constructed from the alignment of 74,389 variable positions found in the concatenated alignment of 4,616 core orthologous genes for the chromosome and 120 variable positions identified in the concatenated alignment of 88 pXO2 core orthologous genes. No signal of plasmid lateral transfer between the two phylogroups was apparent.

Strain CI was more closely related to the *B. anthracis* group than it was to the other *B. cereus* bv. *anthracis* isolates.

Further, clustering based on the presence/absence of the variable genes of both plasmids showed a grouping pattern similar to that of the chromosome (Fig. S4B and E), indicating that (higher) gene content variation largely correlates to (higher) genome

divergence. Collectively, these results indicated limited horizontal transfer of the plasmid between *B. cereus* and *B. anthracis*. Accordingly, *B. cereus* genomes harboring the *B. anthracis* plasmids appear to have maintained these plasmids since their last common ancestor with *B. anthracis*. However, we did observe topological incongruences between the chromosome and pXO1 core gene trees within *B. anthracis* (entanglement = 0.20, Fig. S5A), indicating that the plasmid might have undergone horizontal transfer within the group. For instance, the chromosome-based and plasmid-based topologies were significantly incongruent by all three tests applied, i.e., the one-sided maximum likelihood (ML) Kishino-Hasegawa test (KH) (30), the Shimodaira-Hasegawa test (SH) (31), and the expected likelihood weight test (ELW) (32) ( $p_{1sKH} = 0.005$ ,  $p_{SH} = 0.002$ ,  $c-ELW = 0.002$  [where  $p_{val}$  is  $P$  value,  $1sKH$  is one-sided Kishino-Hasegawa test, and  $c-ELW$  is cumulative expected likelihood weight test]; all tests were applied with a 5% significance level and 1,000 resamplings using the resampling of estimated log-likelihoods [RELL] method). However, further analysis showed that the topological differences mentioned above were predominantly due to recombination and/or varied selection pressures only in genes encoding five products (OG20, a hypothetical protein containing a DUF87 domain; OG149, the Edema factor [*cya*] component in the anthrax toxin; OG39, a type IV secretion system protein; OG133, the protective antigen [*pagA*] in the anthrax toxin; OG135, a germination protein [*gerKC*]) and were not plasmid-wide. When these genes were removed from the core gene alignment, the plasmid tree and the chromosome were topologically more congruent (entanglement = 0.05) (Fig. S5B). We also observed that the complete pXO1 and chromosome trees grouped in the same cluster (less distance between them) in a minimally dimensional representation of the topological variability of the trees evaluated using the Kendall and Colijn metric (Fig. S5C and D) (see Materials and Methods). Collectively, our analyses revealed no strong evidence of plasmid lateral transfer between or within *B. anthracis* and *B. cereus*.

## DISCUSSION

In this study, we estimated plasmid copy numbers in a large collection of newly sequenced *B. anthracis* strains, characterized their full plasmid gene content, and compared the levels of phylogenetic diversity of representative genomes with those of other *Bacillus* species carrying complete or partial pXO1/pXO2-like plasmids. Our major findings showed that *B. anthracis* cells maintain, on average, 3.86 copies of pXO1 and 2.29 copies of pXO2 and revealed that there is a positive linear correlation in the numbers of copies of both plasmids which was consistent with two previously reported sequence-based studies (12, 13). The gene content of these *B. anthracis* plasmids was remarkably stable, although a few genomes (e.g., that of strain 2000031682) lacked large parts of the plasmids. Furthermore, the number of plasmid copies that *B. anthracis* genomes harbored seemed to be influenced by the source from where the strains were isolated (animal or environmental) but not by phylogeny. We also identified several environmental *B. cereus sensu lato* strains containing pXO1-like and pXO2-like contigs, some of which had been previously reported (33). We found no strong evidence of plasmid exchange between *B. anthracis* and *B. cereus sensu lato* genomes, suggesting plasmid maintenance since the last common ancestor of the two species.

Our estimates revealed a lower number of pXO1 copies per chromosome, on average ( $n = 3.86$ ), than had been reported from earlier studies based on molecular methods such as qPCR. For example, Coker et al. estimated ratios of up to 40 copies of pXO1 (8), while Pilo et al. reported 10 to 11 copies of the same plasmid (11). In both cases, the estimation based on quantities of a portion of a single gene per replicon, representing ~0.1% of the total replicon length, seemed to be inflated compared with our more comprehensive shotgun sequence-based estimations. However, for pXO2, qPCR and sequencing provided similar estimates of approximately 1 to 2 copies per cell. This indicated that PCR may have overestimated pXO1 abundance since the competing hypothesis, that sequencing was biased against pXO1 abundance but not against that of pXO2, appears to be less parsimonious. However, we have also identified

strains carrying up to 4.5 copies of pXO2. The fact that the plasmid copy number was not a phylogenetically conserved trait but was influenced by the source of isolation suggested that extrinsic forces (e.g., environmental factors such as temperature, pH, soil moisture, and cation levels, among others) might play a more important role in determining the number of replicons that *B. anthracis* cells maintain. In other words, the plasmid copy number may become adjusted in response to environmental cues. Studies of the ecology of *B. anthracis* have shown that the global distribution of anthrax was largely determined by climatic factors and land features, where, for example, soils with high calcium levels and a pH above 6.1 foster better spore survival (6, 9, 34). It should also be mentioned that although the prevailing assumption was that *B. anthracis* remains primarily dormant in soil as spores, several recent studies have suggested growth in soil/rhizosphere. For example, Saile and Koehler showed that *B. anthracis* strains can germinate on and around roots, suggesting that even environmental strains can grow and be metabolically active under specific conditions (35). Thus, the trend reported here of higher plasmid copy numbers in strains from animal sources, including human tissues, likely reflected a real ecological adaptation between different sources rather than just the effect of prolonged time in the spore stage for environmental strains.

We also characterized the gene content diversity of the plasmids across the set of strains carrying one or both plasmids. Our results confirmed that the highly conserved gene content and synteny for both plasmids (>97% of total plasmid genes shared) were similar to what has been previously described for this species. In addition, we identified a single strain (2000031682) with a large fragment deletion in the pXO1 plasmid. The deleted fragment size was approximately 46.3 kbp, and the fragment carried the main virulence genes responsible for anthrax toxin production: *cya*, *pagA*, *lef*, and *atxA*. While the history of this strain is not clear, it was originally archived at CDC in 1964 on an agar slant and stored at room temperature. The strain was recovered from the slant and frozen at  $-70^{\circ}\text{C}$  in 2001. We previously reported that numerous strains in this collection were cured of plasmids during decades in room temperature storage (36). We cannot ascertain whether this strain was received under this condition or if the deletion might have occurred during storage.

In this study, we also characterized environmental *B. cereus sensu lato* strains possessing partial or complete pXO1/pXO2-like plasmids and *B. cereus* bv. *anthracis* strains possessing complete *B. anthracis* plasmids. Through bioinformatic approaches, we identified 50 strains with contigs homologous to those of pXO1 and/or pXO2. We confirmed that pXO1-like and pXO2-like contigs were widely prevalent in environmental isolates of the *B. cereus sensu lato* group, similarly to what was previously revealed by Van der Auwera et al. using PCR-based approaches (33). The annotation of the genes present in pXO1/pXO2-like contigs showed that most of them were identified as encoding hypothetical proteins, with few of them predicted to be involved in DNA insertion and transposition (for example, retron-type RNA-directed DNAases and ribonucleases; see Fig. 4B), but no genes encoding anthrax toxins were identified. However, we found genes encoding hyaluronic acid (HA) capsule formation in these contigs. An HA capsule provides pathogenic bacilli with capsular material used to escape the innate host immune response and is involved in the pathogenesis of anthrax-like diseases (37, 38). Given that all the *B. cereus sensu lato* strains analyzed here were of environmental origin, these findings might indicate that at least some of the virulence factors encoded on the *B. anthracis* plasmids (e.g., HA capsule formation) may be important for survival in the environment outside the human host.

A potential limitation in our study was the possibility that some strains could have lost part(s) or all of their plasmids during successive subculturing or that their plasmid copy number was adjusted upon cultivation under laboratory conditions compared to the natural environment. The rate of plasmid loss during recurrent subculturing could have been accelerated under laboratory conditions of stress (36) which might potentially have also biased our estimation of the “true” copy number variation. To minimize this issue, the original culture stock, rather than derived subcultures, was used for

preparing DNA for sequencing. To investigate this limitation further, a larger effort with respect to soil/field sampling would be necessary to evaluate how frequently *B. cereus* group strains carry complete or partial pXO1/pXO2-like plasmids and the natural copy number of *B. cereus*/*B. anthracis* strains. The fact that we did observe differences between strains of environmental origin and of clinical origin, even though all strains had been maintained under laboratory conditions since their isolation, further indicated that significant biological/ecological differences likely underlay the plasmid copy number variation observed here.

Phylogenetic reconstruction of *B. anthracis* medoids and the *B. cereus* bv. *anthracis* and human-pathogenic *B. cereus* genomes based on analysis of pXO2 core genes showed that strain CI was more closely related to the members of the *B. anthracis* group than it was to other *B. cereus* bv. *anthracis* strains (see Fig. S4D in the supplemental material). Antonation and colleagues reported that strain CI is closer to other *B. cereus* bv. *anthracis* strains than *B. anthracis*, even though this strain showed the largest intragroup distance to other *B. cereus* bv. *anthracis* members (23). This inconsistency is most likely due to differences between the two studies in the bioinformatic approaches used to build trees. Antonation et al. estimated phylogenetic relationships based on SNP data of core plasmid genes, while our tree was based on the concatenated alignment of core orthologous genes (88 in total).

In summary, by using next-generation sequencing data, we have estimated *B. anthracis* plasmid copy numbers, characterized their genomic diversity, and compared representative strains to clinical and environmental *B. cereus sensu lato* strains carrying pXO1/pXO2-like plasmids. The results derived from this study have advanced our understanding of the biology of the *B. cereus* group, improved the ecological and evolutionary framework used to classify species, and appropriately defined phylogenetic relationships and taxonomic assignments within the *B. cereus sensu lato* group. Our results also highlighted the advantages of using genomic relatedness (as measured by ANI, for example), instead of plasmid-encoded traits, to assign taxonomy and robustly resolve the relationships among closely related members of the *B. cereus sensu lato* group. These results and interpretations were also consistent with previous studies of plasmid-encoded traits in other bacterial species such as *Clostridium botulinum* (39). Therefore, the results derived from our study will help to improve the ecological and evolutionary framework used to classify species and appropriately define phylogenetic relationships, particularly in bacterial groups that exhibit high phenotypic diversity such as the *B. cereus sensu lato* group.

Although the collection size of the *B. anthracis* strains sequenced in this study and the number of strains deposited in public databases are likely still small compared to the total natural diversity of the species, to the best of our knowledge, this is the largest study characterizing *B. anthracis* plasmid copy number variation and gene content diversity using sequencing data to date. Hence, the data presented here should facilitate future studies of *B. anthracis* and its virulence plasmids. Finally, the bioinformatic approaches used in this study can also be applied as a reference framework for epidemiological studies involving this and other microorganisms of medical relevance.

## MATERIALS AND METHODS

**Collection description.** The collection of genomes analyzed in this study is part of the Zoonoses and Select Agent Laboratory's historical strain collection at the Centers for Disease Control and Prevention. The strains included in the study were acquired from human, animal, and environmental sources worldwide from the 1950s to 2013. The complete set has been deposited in the NCBI sequence read archive (SRA) under BioProject identifier (ID) 264742 (see Table S1 in the supplemental material).

**Growth conditions, DNA extraction, and sequencing.** DNA was extracted from isolates using a QIAamp DNA blood Minikit (Qiagen, Valencia, CA) or a Maxwell 16 instrument (Promega, Madison, WI). For the QIAamp extraction, cells were grown overnight in heart infusion broth (Remel, Lenexa, KS). Cells were pelleted by centrifugation for 10 min at  $5,000 \times g$ . Broth was removed, and DNA was extracted using a Qiagen QIAamp DNA blood Minikit and following the manufacturer's protocol for isolating genomic DNA from Gram-positive bacteria. For DNA extractions performed using the Maxwell instrument, the manufacturer's protocol was followed. Briefly, cells were grown overnight on Trypticase soy agar with 5% sheep blood and then mechanically disrupted by vortex mixing for 2 min in a suspension of silica beads and Tris-EDTA (TE) buffer (Promega; Maxwell RSC). The suspension was centrifuged for 30 s

at  $10,000 \times g$ . A 300- $\mu$ l volume of the resulting supernatant was used for DNA extraction following the manufacturer's protocol for blood and cells. Sequencing was performed on an Illumina GAIIx system using TruSeq chemistry.

**Read quality control, assembly, and gene prediction.** Raw reads were initially screened for adaptor sequences using Scythe (40) and trimmed at both the 5' and 3' ends based on a PHRED score cutoff of 20 using SolexaQA++ (41). Reads that were <50 bp in length after trimming were discarded. Quality-filtered reads were *de novo* assembled using IDBA-UD with precorrections (42), and the percentages of contamination and genome completeness were assessed based on either recovery of lineage-specific marker genes using CheckM (43) or recovery of essential genes (single copy) in bacterial and archaeal genomes using the script *HMM.essential.rb* available at the Enveomics collection (44). Protein-coding sequences were predicted using MetaGeneMark (45), and 16S rRNA gene sequences were identified using barnap 0.6 (<https://github.com/tseemann/barnap>). All predicted genes from the assemblies were taxonomically annotated using MyTaxa (46), and the taxonomic distributions of adjacent genes (in windows of 10 genes) in the concatenated assembly were inspected for possible contamination through the use of bar plots. The methods and scripts for read quality control, assembly, and gene prediction described above were used as part of MiGA (Microbial Genomes Atlas), a system developed in our laboratory for data management and processing of microbial genomes and metagenomes (<http://microbial-genomes.org/>).

**B. anthracis and B. cereus sensu lato reference genomes.** Assembled sequencing data for 36 additional *B. anthracis* strains and raw sequencing reads for 130 *B. cereus sensu lato* reference strains were downloaded from the nucleotide database or the sequencing read archive (SRA) at NCBI (<https://www.ncbi.nlm.nih.gov/sra>) with the accession numbers listed in Table S2. Reference strains were processed in parallel with the CDC *B. anthracis* collection as described above. After quality control inspection, 26 *B. cereus* reference strains showing  $\geq 20\%$  contamination as calculated with CheckM (see above) were excluded from the analysis.

**Plasmid copy number estimation.** Whole-genome sequencing enabled estimation of the copy number of each plasmid relative to the number of chromosome copies in each sequence library. Copy number was estimated as the ratio of the average sequencing depth across the whole plasmid sequence to the average sequencing depth across the chromosome. The effects of short regions with very high or very low sequencing depth on average sequencing depth were negligible. To speed up computational processing, read sets were randomly subsampled to a level where conclusions would not change. After creating various library sizes, we calculated the pXO1 copy number for three libraries of different sizes (large, medium, and small), and a level of as little as 10% of the library size did not have an effect in copy number estimation (see Fig. S1 in the supplemental material). Quality-filtered sequence libraries were therefore subsampled to 10% of their size and blastn mapped to three targets: the reference *B. anthracis* Ames ancestor (GCF\_000008445.1), plasmids pXO1 (NC\_007322.2) and pXO2 (NC\_007323.2), and each assembled genome. Read depths were calculated for each library using the function "enve.recpilot" incorporated in the R package "enveomics.R" (44). Using the same R function, read recruitment plots were generated for each library to quantify and visualize the coverage across the full length of the reference plasmids to determine the presence/absence of the entire plasmid. Presence data were considered true if the calculated average sequencing depth across the full reference was  $\geq 2\times$  in the subsampled library.

**Average nucleotide identity (ANI) distances and medoids.** The average nucleotide identity (ANI) (47, 48) between the sets of genomes was calculated using the command line interface of MiGA (Microbial Genome Atlas; <https://github.com/bio-miga/miga>). Briefly, MiGA calculated a matrix of distances with  $1 - \text{ANI}$  for all pairs of genomes considered in the database. Subsequently, clusters in the matrix were identified using the PAM algorithm (partitioning around the medoids) (49) with  $k$  medoids, where  $k$  was determined by the local gain in the average Silhouette width (50) for each level of clustering until a group of five or fewer genomes was reached. Here, the medoids were representative strains in the diversity space. Afterward, a dendrogram was built based on ANI distances ( $1 - \text{ANI}$ ) using hierarchical agglomerative clustering with the Ward criterion (26).

**Phylogenetic signal in plasmid copy number.** Phylogenetic conservatism of plasmid copy numbers was determined through the calculation of the Blomberg's  $K$  statistic (51) included in the function "phylosignal" of the R package "Picante" (52).  $K$  values of 1 correspond to a Brownian motion process, which implies some degree of phylogenetic signal or conservatism.  $K$  values closer to zero correspond to a random or convergent pattern of evolution, while  $K$  values greater than 1 indicate strong phylogenetic signal and conservatism of traits.

**Phylogenomic relationship of plasmids and chromosome based on ANI.** Large ( $\geq 500$ -bp) contigs with  $\geq 80\%$  identity and  $\geq 80\%$  query coverage with respect to either pXO1 or pXO2 *B. anthracis* Ames ancestor reference sequences were considered to be pXO1 or pXO2 homologous and were extracted from the assemblies. Dendrograms based on ANI distances were built for the plasmids and chromosomes as described previously and subsequently compared through tanglegrams using the R package *Dendextend*, version 1.2.0 (53). Statistical correlation between pairs of dendrograms was evaluated with two parameters: Baker's  $\Omega$  index correlation (54) and the cophenetic distant correlation (55). Both are included in the R package *Dendextend*.

**Read-based genomic gene content analysis.** pXO1 and pXO2 ortholog genes among *B. anthracis* genomes were identified using a reciprocal-best match (RBM) blastn approach as described by Weigand et al. (39). In brief, the sequences of the predicted genes in the plasmid sequence of one strain were searched against the predicted genes of all of the remaining strains in the set in a pairwise fashion using blastn (56). Reciprocal best matches were identified when the best match was bidirectional for the pair of strains being compared and when there was at least 70% nucleotide identity and 70% query gene

coverage using *rbm.rb* (44). Next, orthologous groups (OGs) in reciprocal best matches were identified using the unsupervised Markov cluster algorithm (MCL) implemented in *ogs.mcl.rb* in the Enveomics collection (44) with the following default settings: 1.5 inflation parameter and bit score as parameter to weight edges. Descriptive statistics on the set of orthology groups were estimated using the script *ogs.stats.rb* (Enveomics collection). Genes conserved in all genomes were identified as core orthologous genes. Genes conserved in some but not all of the strains were identified as variable orthologous genes. Representative orthologous genes from the previous analysis (including both core and variable genes) were randomly selected and extracted to generate a pangenome or “bag of genes.” To better determine the presence/absence of the genes included in the pangenome, we recruited raw sequencing reads against the predicted genes on the plasmid. For this, FastA libraries were subsampled to 500,000 reads per sample and mapped against the set of representative orthologous genes using *blastn*. The maximum number of target sequences in the database was set to 1 (best match). The observed and estimated sequencing depths as well as the number of reads mapping to each gene in the database were calculated using the script “*BlastTab.seqdepth\_ZIP.pl*” from the Enveomics collection (44), assuming a zero-inflated Poisson distribution to correct for noncovered positions with parameters estimated as described by Beckett et al. (57). Orthologous genes with zero inflation values of  $\geq 0.3$ , which represent the fraction of the gene that is not covered, were excluded. Thus, only genes with  $\geq 70\%$  coverage were considered to be present. The calculated average sequencing depths for the genes in pXO1 were  $32.2\times$  and  $19.9\times$  for the genes in pXO2. To determine the copy number of the genes in each plasmid, the sequencing depth calculated for each gene in each strain was normalized by the median sequencing depth of each strain and reported through a dendrogram of hierarchical clustering.

**Genomic characterization of *B. anthracis* and *B. cereus* strains carrying pXO1-like and/or pXO2-like plasmids.** Orthologous genes among *B. anthracis* medoids and *B. cereus* genomes carrying *B. anthracis*-like plasmids were identified through the reciprocal-best match (RBM) *blastn* approach as described above. Core genes were extracted and aligned to estimate phylogenetic relationships between *B. cereus* and *B. anthracis*. The sets of core genes were filtered to remove in-paralogous genes and aligned using MUSCLE v3.8.31 (58) with default parameters. The aligned outputs were saved in FastA format, and the script *Aln.cat.rb* from the Enveomics collection was used to concatenate the multiple alignments into a single file and to remove invariable sites, defined as columns with only one state and undefined characters. Phylogenetic reconstructions were performed with either RAxML version 8.1.21 (59) or FastTree version 2.1.7 (60) with the GTR model for nucleotides used in both cases. The collection of variable genes, defined as genes absent in 1 or more genomes, was identified as described above. The presence or absence of these variable genes was used to cluster genomes hierarchically using a complete linkage across a centered Pearson correlation similarity range using the function “*heatmap2*” contained in the R package *gplots* v3.0.1 (<https://CRAN.R-project.org/package=gplots>). Functional annotation of variable genes was bioinformatically inferred through a BLASTP search against the RefSeq protein and the UniProtKB/Swiss-Prot databases with identity greater than 45% and minimal query coverage of 70%.

Tests for incongruence between phylogenetic trees were performed using TREE-PUZZLE 5.2 and maximum likelihood (ML) (61). ML analysis was carried out using empirically derived base frequencies, ratios of transitions to transversions estimated from data sets, the HKY model of substitution, a gamma distribution model for site rate variation with  $\alpha$ -parameter estimated from data set, and 4 gamma rate categories. Topological variability or distances among trees derived from individual OGs were calculated using the Kendall and Colijn metric (62) implemented in R package “*treeSpace*” (63). Tanglegram entanglements were calculated as described previously (53).

**Data availability.** The complete set of strains sequenced in this study has been deposited in the NCBI Sequence Read Archive (SRA) under BioProject ID [264742](https://www.ncbi.nlm.nih.gov/bioproject/264742) (see Table S1 for strain-specific accession numbers).

## SUPPLEMENTAL MATERIAL

Supplemental material for this article may be found at <https://doi.org/10.1128/mSystems.00065-18>.

**FIG S1**, EPS file, 0.4 MB.

**FIG S2**, EPS file, 1.6 MB.

**FIG S3**, EPS file, 2.9 MB.

**FIG S4**, EPS file, 2.6 MB.

**FIG S5**, EPS file, 2.3 MB.

**FIG S6**, EPS file, 0.8 MB.

**TABLE S1**, DOCX file, 0.1 MB.

**TABLE S2**, XLSX file, 0.1 MB.

**TABLE S3**, XLSX file, 0.04 MB.

## ACKNOWLEDGMENTS

The findings and conclusions in this report are ours and do not necessarily represent the official position of the Centers for Disease Control and Prevention (CDC). Mention of company names or products does not constitute endorsement by the CDC.

This work was supported by United States National Science Foundation award



number 1356288 and DHHS/PHS/CDC award no. RF023 to K.T.K. A.P.-G. was partially supported by Colciencias—Colombian Administrative Department for Science, Technology and Innovation—through a doctoral fellowship.

## REFERENCES

- Derzelle S, Girault G, Kokotovic B, Angen Ø. 2015. Whole genome-sequencing and phylogenetic analysis of a historical collection of *Bacillus anthracis* strains from Danish cattle. *PLoS One* 10:e0134699. <https://doi.org/10.1371/journal.pone.0134699>.
- Van Ert MN, Easterday WR, Huynh LY, Okinaka RT, Hugh-Jones ME, Ravel J, Zanecki SR, Pearson T, Simonson TS, U'Ren JM, Kachur SM, Leadem-Dougherty RR, Rhoton SD, Zinser G, Farlow J, Coker PR, Smith KL, Wang B, Kenefic LJ, Fraser-Liggett CM, Wagner DM, Keim P. 2007. Global genetic population structure of *Bacillus anthracis*. *PLoS One* 2:e461. <https://doi.org/10.1371/journal.pone.0000461>.
- Girault G, Blouin Y, Vergnaud G, Derzelle S. 2014. High-throughput sequencing of *Bacillus anthracis* in France: investigating genome diversity and population structure using whole-genome SNP discovery. *BMC Genomics* 15:288. <https://doi.org/10.1186/1471-2164-15-288>.
- Hendricks KA, Wright ME, Shadomy SV, Bradley JS, Morrow MG, Pavia AT, Rubinstein E, Holty JC, Messonnier NE, Smith TL, Pesik N, Treadwell TA, Bower WA. 2014. Centers for Disease Control and Prevention expert panel meetings on prevention and treatment of anthrax in adults. *Emerg Infect Dis* 20:e130687. <https://doi.org/10.3201/eid2002.130687>.
- Pilo P, Frey J. 2011. *Bacillus anthracis*: molecular taxonomy, population genetics, phylogeny and patho-evolution. *Infect Genet Evol* 11:1218–1224. <https://doi.org/10.1016/j.meegid.2011.05.013>.
- Hugh-Jones M, Blackburn J. 2009. The ecology of *Bacillus anthracis*. *Mol Aspects Med* 30:356–367. <https://doi.org/10.1016/j.mam.2009.08.003>.
- Riojas MA, Kiss K, McKee ML, Hazzbón MH. 2015. Multiplex PCR for species-level identification of *Bacillus anthracis* and detection of pXO1, pXO2, and related plasmids. *Health Sec* 13:122–129. <https://doi.org/10.1089/hs.2014.0056>.
- Coker PR, Smith KL, Fellows PF, Rybachuck G, Kousoulas KG, Hugh-Jones ME. 2003. *Bacillus anthracis* virulence in guinea pigs vaccinated with anthrax vaccine adsorbed is linked to plasmid quantities and clonality. *J Clin Microbiol* 41:1212–1218. <https://doi.org/10.1128/JCM.41.3.1212-1218.2003>.
- Bergman NH (ed). 2011. *Bacillus anthracis* and anthrax. John Wiley & Sons, Hoboken, NJ.
- Irengue LM, Gala JL. 2012. Rapid detection methods for *Bacillus anthracis* in environmental samples: a review. *Appl Microbiol Biotechnol* 93:1411–1422. <https://doi.org/10.1007/s00253-011-3845-7>.
- Pilo P, Rossano A, Bamanga H, Abdoukadiiri S, Perreten V, Frey J. 2011. Bovine *Bacillus anthracis* in Cameroon. *Appl Environ Microbiol* 77:5818–5821. <https://doi.org/10.1128/AEM.00074-11>.
- Straub T, Baird C, Bartholomew RA, Colburn H, Seiner D, Victry K, Zhang L, Bruckner-Lea CJ. 2013. Estimated copy number of *Bacillus anthracis* plasmids pXO1 and pXO2 using digital PCR. *J Microbiol Methods* 92:9–10. <https://doi.org/10.1016/j.mimet.2012.10.013>.
- Ravel J, Jiang L, Stanley ST, Wilson MR, Decker RS, Read TD, Worsham P, Keim PS, Salzberg SL, Fraser-Liggett CM, Rasko DA. 2009. The complete genome sequence of *Bacillus anthracis* Ames “Ancestor”. *J Bacteriol* 191:445–446. <https://doi.org/10.1128/JB.01347-08>.
- Papazisi L, Rasko DA, Ratnayake S, Bock GR, Remortel BG, Appalla L, Liu J, Dracheva T, Braisted JC, Shallom S, Jarrahi B, Snesrud E, Ahn S, Sun Q, Rilstone J, Okstad OA, Kolstø AB, Fleischmann RD, Peterson SN. 2011. Investigating the genome diversity of *B. cereus* and evolutionary aspects of *B. anthracis* emergence. *Genomics* 98:26–39. <https://doi.org/10.1016/j.ygeno.2011.03.008>.
- Okinaka RT, Keim P. 2016. The phylogeny of *Bacillus cereus* sensu lato. *Microbiology Spectrum* 4. <https://doi.org/10.1128/microbiolspec.TBS-0012-2012>.
- Økstad OA, Kolstø A-B. 2011. Genomics of bacillus species, p 29–53. *In* Genomics of foodborne bacterial pathogens. Springer, Berlin, Germany.
- Granum PE, Lund T. 1997. *Bacillus cereus* and its food poisoning toxins. *FEMS Microbiol Lett* 157:223–228. <https://doi.org/10.1111/j.1574-6968.1997.tb12776.x>.
- Helgason E, Caugant DA, Olsen I, Kolstø AB. 2000. Genetic structure of population of *Bacillus cereus* and *B. thuringiensis* isolates associated with periodontitis and other human infections. *J Clin Microbiol* 38:1615–1622.
- Maughan H, Van der Auwera G. 2011. *Bacillus* taxonomy in the genomic era finds phenotypes to be essential though often misleading. *Infect Genet Evol* 11:789–797. <https://doi.org/10.1016/j.meegid.2011.02.001>.
- Marston CK, Ibrahim H, Lee P, Churchwell G, Gumke M, Stanek D, Gee JE, Boyer AE, Gallegos-Candela M, Barr JR, Li H, Boulay D, Cronin L, Quinn CP, Hoffmaster AR. 2016. Anthrax toxin-expressing *Bacillus cereus* isolated from an anthrax-like eschar. *PLoS One* 11:e0156987. <https://doi.org/10.1371/journal.pone.0156987>.
- Hoffmaster AR, Ravel J, Rasko DA, Chapman GD, Chute MD, Marston CK, De BK, Sacchi CT, Fitzgerald C, Mayer LW, Maiden MC, Priest FG, Barker M, Jiang L, Cer RZ, Rilstone J, Peterson SN, Weyant RS, Galloway DR, Read TD, Popovic T, Fraser CM. 2004. Identification of anthrax toxin genes in a *Bacillus cereus* associated with an illness resembling inhalation anthrax. *Proc Natl Acad Sci U S A* 101:8449–8454. <https://doi.org/10.1073/pnas.0402414101>.
- Hoffmaster AR, Hill KK, Gee JE, Marston CK, De BK, Popovic T, Sue D, Wilkins PP, Avashia SB, Drumgoole R, Helma CH, Ticknor LO, Okinaka RT, Jackson PJ. 2006. Characterization of *Bacillus cereus* isolates associated with fatal pneumonias: strains are closely related to *Bacillus anthracis* and harbor *B. anthracis* virulence genes. *J Clin Microbiol* 44:3352–3360. <https://doi.org/10.1128/JCM.00561-06>.
- Antonation KS, Grützmacher K, Dupke S, Mabon P, Zimmermann F, Lankester F, Peller T, Feistner A, Todd A, Herbingler I, de Nys HM, Muyembe-Tamfun JJ, Karhemere S, Wittig RM, Couacy-Hymann E, Grunow R, Calvignac-Spencer S, Corbett CR, Klee SR, Leendertz FH. 2016. *Bacillus cereus* biovar anthracis causing anthrax in sub-Saharan Africa—chromosomal monophyly and broad geographic distribution. *PLoS Negl Trop Dis* 10:e0004923. <https://doi.org/10.1371/journal.pntd.0004923>.
- Klee SR, Özel M, Appel B, Boesch C, Ellerbrok H, Jacob D, Holland G, Leendertz FH, Pauli G, Grunow R, Nattermann H. 2006. Characterization of *Bacillus anthracis*-like bacteria isolated from wild great apes from Cote d'Ivoire and Cameroon. *J Bacteriol* 188:5333–5344. <https://doi.org/10.1128/JB.00303-06>.
- Pena-Gonzalez A, Marston CK, Rodriguez-R LM, Kolton CB, Garcia-Diaz J, Theppote A, Frace M, Konstantinidis KT, Hoffmaster AR. 2017. Draft genome sequence of *Bacillus cereus* LA2007, a human-pathogenic isolate harboring anthrax-like plasmids. *Genome Announc* 5:e00181-17. <https://doi.org/10.1128/genomeA.00181-17>.
- Murtagh F, Legendre P. 2014. Ward's hierarchical agglomerative clustering method: which algorithms implement ward's criterion? *J Classif* 31:274–295. <https://doi.org/10.1007/s00357-014-9161-z>.
- Zwick ME, Joseph SJ, Didelot X, Chen PE, Bishop-Lilly KA, Stewart AC, Willner K, Nolan N, Lentz S, Thomason MK, Sozhamannan S, Mateczun AJ, Du L, Read TD. 2012. Genomic characterization of the *Bacillus cereus* sensu lato species: backdrop to the evolution of *Bacillus anthracis*. *Genome Res* 22:1512–1524. <https://doi.org/10.1101/gr.134437.111>.
- Tourasse NJ, Kolstø AB. 2008. SuperCAT: a supertree database for combined and integrative multilocus sequence typing analysis of the *Bacillus cereus* group of bacteria (including *B. cereus*, *B. anthracis* and *B. thuringiensis*). *Nucleic Acids Res* 36:D461–D468. <https://doi.org/10.1093/nar/gkm877>.
- Tourasse NJ, Helgason E, Økstad OA, Hegna IK, Kolstø AB. 2006. The *Bacillus cereus* group: novel aspects of population structure and genome dynamics. *J Appl Microbiol* 101:579–593. <https://doi.org/10.1111/j.1365-2672.2006.03087.x>.
- Kishino H, Hasegawa M. 1989. Evaluation of the maximum likelihood estimate of the evolutionary tree topologies from DNA sequence data, and the branching order in Hominoidae. *J Mol Evol* 29:170–179. <https://doi.org/10.1007/BF02100115>.
- Shimodaira H, Hasegawa M. 1999. Multiple comparisons of log-likelihoods with applications to phylogenetic inference. *Mol Biol Evol* 16:1114–1116. <https://doi.org/10.1093/oxfordjournals.molbev.a026201>.
- Strimmer K, Rambaut A. 2002. Inferring confidence sets of possibly

- misspecified gene trees. *Proc Biol Sci* 269:137–142. <https://doi.org/10.1098/rspb.2001.1862>.
33. Van der Auwera GA, Feldgarden M, Kolter R, Mahillon J. 2013. Whole-genome sequences of 94 environmental isolates of *Bacillus cereus* sensu lato. *Genome Announc* 1:e00380-13. <https://doi.org/10.1128/genomeA.00380-13>.
  34. World Health Organization, International Office of Epizootics. 2008. Anthrax in humans and animals. World Health Organization, Geneva, Switzerland.
  35. Saile E, Koehler TM. 2006. *Bacillus anthracis* multiplication, persistence, and genetic exchange in the rhizosphere of grass plants. *Appl Environ Microbiol* 72:3168–3174. <https://doi.org/10.1128/AEM.72.5.3168-3174.2006>.
  36. Marston CK, Hoffmaster AR, Wilson KE, Bragg SL, Plikaytis B, Brachman P, Johnson S, Kaufmann AF, Popovic T. 2005. Effects of long-term storage on plasmid stability in *Bacillus anthracis*. *Appl Environ Microbiol* 71:7778–7780. <https://doi.org/10.1128/AEM.71.12.7778-7780.2005>.
  37. Brézillon C, Haustant M, Dupke S, Corre JP, Lander A, Franz T, Monot M, Couture-Tosi E, Jouvion G, Leendertz FH, Grunow R, Mock ME, Klee SR, Goossens PL. 2015. Capsules, toxins and AtxA as virulence factors of emerging *Bacillus cereus* biovar anthracis. *PLoS Neglect Trop Dis* 9:e0003455. <https://doi.org/10.1371/journal.pntd.0003455>.
  38. Oh SY, Budzik JM, Garufi G, Schneewind O. 2011. Two capsular polysaccharides enable *Bacillus cereus* G9241 to cause anthrax-like disease. *Mol Microbiol* 80:455–470. <https://doi.org/10.1111/j.1365-2958.2011.07582.x>.
  39. Weigand MR, Pena-Gonzalez A, Shirey TB, Broeker RG, Ishaq MK, Konstantinidis KT, Raphael BH. 2015. Implications of genome-based discrimination between *Clostridium botulinum* group I and *Clostridium sporogenes* strains for bacterial taxonomy. *Appl Environ Microbiol* 81:5420–5429. <https://doi.org/10.1128/AEM.01159-15>.
  40. Buffalo V. 2014. Scythe—a Bayesian adapter trimmer (version 0.994 beta). <https://github.com/vsbuffalo/scythe>.
  41. Cox MP, Peterson DA, Biggs PJ. 2010. SolexaQA: at-a-glance quality assessment of Illumina second-generation sequencing data. *BMC Bioinformatics* 11:485. <https://doi.org/10.1186/1471-2105-11-485>.
  42. Peng Y, Leung HCM, Yiu SM, Chin FYL. 2012. IDBA-UD: a de novo assembler for single-cell and metagenomic sequencing data with highly uneven depth. *Bioinformatics* 28:1420–1428. <https://doi.org/10.1093/bioinformatics/bts174>.
  43. Parks DH, Imelfort M, Skennerton CT, Hugenholtz P, Tyson GW. 2015. CheckM: assessing the quality of microbial genomes recovered from isolates, single cells, and metagenomes. *Genome Res* 25:1043–1055. <https://doi.org/10.1101/gr.186072.114>.
  44. Rodriguez LM, Konstantinidis KT. 2016. The enveomics collection: a toolbox for specialized analyses of microbial genomes and metagenomes. *PeerJ Preprints* 4:e1900v1. <https://peerj.com/preprints/1900/>.
  45. Lukashin AV, Borodovsky M. 1998. GeneMark.hmm: new solutions for gene finding. *Nucleic Acids Res* 26:1107–1115. <https://doi.org/10.1093/nar/26.4.1107>.
  46. Luo C, Rodriguez-R LM, Konstantinidis KT. 2014. MyTaxa: an advanced taxonomic classifier for genomic and metagenomic sequences. *Nucleic Acids Res* 42:e73.
  47. Goris J, Konstantinidis KT, Klappenbach JA, Coenye T, Vandamme P, Tiedje JM. 2007. DNA-DNA hybridization values and their relationship to whole-genome sequence similarities. *Int J Syst Evol Microbiol* 57:81–91. <https://doi.org/10.1099/ijs.0.64483-0>.
  48. Konstantinidis KT, Tiedje JM. 2005. Towards a genome-based taxonomy for prokaryotes. *J Bacteriol* 187:6258–6264. <https://doi.org/10.1128/JB.187.18.6258-6264.2005>.
  49. Kaufman L, Rousseeuw PJ. 1990. Partitioning around medoids (program pam), p 68–125. *Finding groups in data: an introduction to cluster analysis statistics*. John Wiley & Sons, Hoboken, NJ. <https://doi.org/10.1002/9780470316801.ch2>.
  50. Rousseeuw PJ. 1987. Silhouettes: a graphical aid to the interpretation and validation of cluster analysis. *J Comp Appl Math* 20:53–65. [https://doi.org/10.1016/0377-0427\(87\)90125-7](https://doi.org/10.1016/0377-0427(87)90125-7).
  51. Blomberg SP, Garland T, Jr, Ives AR. 2003. Testing for phylogenetic signal in comparative data: behavioral traits are more labile. *Evolution* 57:717–745. <https://doi.org/10.1111/j.0014-3820.2003.tb00285.x>.
  52. Kembel SW, Cowan PD, Helmus MR, Cornwell WK, Morlon H, Ackerly DD, Blomberg SP, Webb CO. 2010. Picante: R tools for integrating phylogenies and ecology. *Bioinformatics* 26:1463–1464. <https://doi.org/10.1093/bioinformatics/btq166>.
  53. Galili T. 2015. Dendextend: an R package for visualizing, adjusting and comparing trees of hierarchical clustering. *Bioinformatics* 31:3718–3720. <https://doi.org/10.1093/bioinformatics/btv428>.
  54. Baker FB. 1974. Stability of two hierarchical grouping techniques case I: sensitivity to data errors. *J Am Stat Assoc* 69:440–445. <https://doi.org/10.1080/01621459.1974.10482971>.
  55. Sokal RR, Rohlf FJ. 1962. The comparison of dendrograms by objective methods. *Taxon* 11:33–40. <https://doi.org/10.2307/1217208>.
  56. Altschul SF, Gish W, Miller W, Myers EW, Lipman DJ. 1990. Basic local alignment search tool. *J Mol Biol* 215:403–410. [https://doi.org/10.1016/S0022-2836\(05\)80360-2](https://doi.org/10.1016/S0022-2836(05)80360-2).
  57. Beckett S, Jee J, Ncube T, Pompilus S, Washington Q, Singh A, Pal N. 2014. Zero-inflated Poisson (ZIP) distribution: parameter estimation and applications to model data from natural calamities. *Involve*. *Involve* 7:751–767. <https://projecteuclid.org/euclid.involve/1513733747>.
  58. Edgar RC. 2004. MUSCLE: a multiple sequence alignment method with reduced time and space complexity. *BMC Bioinformatics* 5:113. <https://doi.org/10.1186/1471-2105-5-113>.
  59. Stamatakis A. 2014. RAxML version 8: a tool for phylogenetic analysis and post-analysis of large phylogenies. *Bioinformatics* 30:1312–1313. <https://doi.org/10.1093/bioinformatics/btu033>.
  60. Price MN, Dehal PS, Arkin AP. 2010. FastTree 2—approximately maximum-likelihood trees for large alignments. *PLoS One* 5:e9490. <https://doi.org/10.1371/journal.pone.0009490>.
  61. Schmidt HA, Strimmer K, Vingron M, Von Haeseler A. 2002. TREE-PUZZLE: maximum likelihood phylogenetic analysis using quartets and parallel computing. *Bioinformatics* 18:502–504. <https://doi.org/10.1093/bioinformatics/18.3.502>.
  62. Kendall M, Colijn C. 2016. Mapping phylogenetic trees to reveal distinct patterns of evolution. *Mol Biol Evol* 33:2735–2743. <https://doi.org/10.1093/molbev/msw124>.
  63. Jombart T, Kendall M, Almagro-Garcia J, Colijn C. 2017. TREESPACE: statistical exploration of landscapes of phylogenetic trees. *Mol Ecol Resour* 17:1385–1392. <https://doi.org/10.1111/1755-0998.12676>.